Preprints (www.preprints.org) | NOT PEER-REVIEWED | Posted: 20 April 2018 doi:10.20944/preprints201804.0257.v1

Article

Trace gas retrieval from AIUS: Algorithm description and O_3 retrieval assessment

Xiaoying Li[1], Tianhai Cheng[1,*] Jian Xu[2,*], Hailiang Shi[3], Xingying Zhang[4], Shule Ge[5], Mingmin Zou[1], Hongmei Wang[1], Yapeng Wang[1], Songyan Zhu[1] and Jing Miao[1]

1. State Key Laboratory of Remote Sensing Science, Institute of Remote Sensing and Digital Earth, Chinese Academy of Sciences, Beijing 100101, China; lixy01@radi.ac.cn (X.L.)
2. Remote Sensing Technology Institute, German Aerospace Center (DLR), Oberpfaffenhofen, Germany
3. Anhui Institute of Optics and Fine Mechanics, Chinese Academy of Sciences, Hefei, Anhui, 230031, China
4. National Satellite Meteorological Center，China Meteorological Administration
5. China Center for Resources Satellite Data and Application, China

* Correspondence: chength@radi.ac.cn (T.C.), jian.xu@dlr.de (J.X.)

Abstract: AIUS (Atmospheric Infrared Ultraspectral Sounder) is an infrared occultation spectrometer onboard the Chinese GaoFen-5 satellite, which covers a spectral range of 2.4--13.3 μm (750--4100 cm^{-1}) with a spectral resolution of about 0.02 cm^{-1}. AIUS is designed to measure and study chemical processes of ozone (O_3) and other trace gases in the upper troposphere and stratosphere around Antarctic. In this study, the corresponding retrieval methodology is described. The retrieval simulations based on the simulated spectra of AIUS have been carried out, with a focus on O_3. The relative difference between the retrieved and the true O_3 profiles is within 5% from the 15km to 70km and about 10% below 15km. The corresponding averaging kernels illustrate that the overall retrieval information mainly come from the spectra, not the a priori. The retrieval experiments also demonstrate that the shape of the retrieved profiles resembles the shape of the true profile even if the shape of the a priori profile is different from that of the true profile. Further, we perform the O_3 retrieval from the real ACE-FTS (Atmospheric Chemistry Experiment-Fourier Transform Spectrometer) measurements and compare the results with the official ACE-FTS Level-2 products. Overall, both profiles agree well in the stratosphere where the retrieval sensitivity is high. The relative difference between both profiles is about 15% below 70km, which may due to the measurement errors and different forward model parameters.

Keywords: AIUS; Occultation; Retrieval algorithm; Microwindows; Ozone

1. Introduction

The annual occurrence of the Antarctic ozone hole has been well documented. For studying ozone recovery, many efforts have been made to understand the chemical and dynamical processes around Antarctic [1-3]. Occultation and limb sounding techniques have provided an important way for remotely observing Earth's middle atmosphere. These measurements have greatly promoted our understanding of the chemical process of atmospheric composition in the upper troposphere and stratosphere by providing profiles measurments with different altitudes. As compared to nadir-viewing measurements, occultation/limb sounding measurements have higher vertical resolution, which can be used to derive vertical information of atmospheric components. Furthermore, high-resolution atmospheric mid-infrared spectra are suitable for detection of many trace species, since a wide variety of vibrational-rotational bands with molecular absorption lines are found within this spectral range. Recently, many occultation observation/limb sounding sensors have been developed and provided abundant profiles of trace gases, such as O_3, CO, H_2O, NO, etc [4–9].

© 2018 by the author(s). Distributed under a Creative Commons CC BY license.

Preprints (www.preprints.org) | NOT PEER-REVIEWED | Posted: 20 April 2018 doi:10.20944/preprints201804.0257.v1

AIUS is one of six payloads onboard the Chinese GaoFen-5 satellite that is expected to launch in May, 2018. AIUS is the first occultation spectrometer developed in China, which is designed to detect the trace gases over the Antarctic. AIUS will operate in a solar synchronous orbit, with a nominal height of 700 km. The instrument is a Fourier transform infrared spectrometer and its main objective is to measure the O_3 and other species in the stratosphere and upper troposphere in order to study the ozone change over the Antarctic.

The aim of this study is to introduce the trace gas retrieval algorithm developed for AIUS and to assess its performance based on ozone retrievals. In Section 2, the instrument parameters and level 1 processing of AIUS are introduced briefly. Section 3 describes the retrieval algorithm in detail. Integrated atmosphere profiles dataset is presented and a sensitivity analysis of atmosphere profiles is showed in Section 4. In Section 5, the simulated spectra and the ACE-FTS observation spectra are adopted to retrieve O_3 profiles and to assess the retrieval performance.

2. AIUS instrument

AIUS is a Fourier transform infrared spectrometer for the detection of occultation transmittance spectra in the middle and upper atmosphere, which has similar characteristics to ACE-FTS. Both instruments have a spectral resolution of 0.02 cm^{-1}. AIUS covers the spectral range from 750 cm^{-1} to 4100 cm^{-1}, while ACE-FTS covers 750--4400 cm^{-1}. It is a dual-band system composed of MCT (mercury cadmium telluride, 750--1850 cm^{-1}) and InSb (1850--4160 cm^{-1}). AIUS covers an altitude range from 8 to 100 km and has a field of view of 1.25 mrad. The latitude coverage of AIUS measurements is about 55° S to 90° S, which is mostly over Antarctica.

GF5-AIUS level 0 is original auxiliary and interferogram data in binary format and level 1 is HDF5 format file includes reconstructed spectra and processed auxiliary data. GF5-AIUS level 0 to level 1 processing includes three steps. The first step is the acquisition and processing of auxiliary data. By unpacketizing the auxiliary data package, the information of observation, such as acquisition time, sun position and satellite position, is acquired. The geometric parameters, the height and the latitude and longitude coordinates, are calculated from the information of the sun and satellite. The second step is to reconstruct the spectra from the original interferogram. However, since the AIUS is an interferometer, the interferogram will contain some spikes produced by the effect of energetic particles due to space electromagnetic environment on orbit, which will contaminate the complete spectra. Thus, some processes have to be involved to correct these errors. The nonlinear behavior of the detectors is expected and characterized on-ground, which requires an additional correction. This nonlinearity correction will be consolidated in-flight using commissioning phase data. After that, the FFT is performed to compute the spectra. The last step is to evaluate the spectra's quality by standard deviation or mean value of imaginary part of the calculated spectra and then make the mark to show if the spectra is well reconstructed. "0" is for good quality and "1" for bad quality.

Level 1 data is the spectra data which are the relative intensities of each tangent heights using DN (digital number) values. Our inversion takes the transmittance converted from the Level 1 data. In addition to the observation of the Sun outside and inside the atmosphere, GF5-AIUS also observes the deep space to remove the instrumental emission. Commonly, the transmittance $\tau(h,\lambda)$ at tangent point h of wave number λ can be calculated by the following equation:

$$\tau(h,\lambda) = \frac{D(h,\lambda)-B(\lambda)}{S(\lambda)-B(\lambda)}, \quad (1)$$

Where $D(h,\lambda)$, $S(\lambda)$ and $B(\lambda)$ are the digital counts of the observation of signal at tangent point h, the solar radiation outside atmosphere and the deep space signal.

3. Retrieval methodology of AIUS

Accurate knowledge of pointing and p/T information is important to high-precision quantitative retrieval of abundances of atmospheric species from occultation observed transmittances. The tangent height correction for AIUS is carried out by employing the triangular

Preprints (www.preprints.org) | NOT PEER-REVIEWED | Posted: 20 April 2018 doi:10.20944/preprints201804.0257.v1

iteration with tangential strides technique in a microwindow of N_2 continuum absorption, whereas the scheme of p/T retrieval is by introducing the hydrostatic equation into the iterative process of optimal algorithm. Details of the design and development of these two algorithms are introduced in our other two papers in preparation.

3.1. Inversion model

The inversion algorithm employed in this study is based on OEM (Optimal Estimation Method) proposed by Rodgers [10]. Since OEM is generally applicable and facilitates a theoretical error analysis, this method has been widely used in the inversion of atmospheric state parameters using infrared and microwave remote sensing measurements, with nadir, occultation or limb viewing [11-16]. OEM stabilizes the inversion process by taking into account the statistical information about the atmospheric variability, which has been investigated by many studies [17-23].

Our inversion scheme is adapted from the retrieval software Qpack 2.0 [23] that uses LM (Levenberg—Marquardt) approach for a nonlinear least squares fitting. The LM iteration method adopted in the Qpack is the same as the LM iteration method modified by Rodgers [17]. By introducing a constraint factor γ, the next iterate is yielded by:

$$\boldsymbol{X}_{i+1} = \boldsymbol{X}_i + [(1+\gamma)\boldsymbol{S}_a^{-1} + \boldsymbol{K}_i^T \cdot \boldsymbol{S}_e^{-1} \cdot \boldsymbol{K}_i]^{-1} \cdot \{\boldsymbol{K}_i^T \boldsymbol{S}_e^{-1}[\boldsymbol{Y} - \boldsymbol{F}(X)] - \boldsymbol{S}_a^{-1}[\boldsymbol{X}_i - \boldsymbol{X}_a]\}. \quad (2)$$

The inverse of the solution covariance in equation (2) is given by:

$$\boldsymbol{S}_x^{-1} = \boldsymbol{K}^T \cdot \boldsymbol{S}_e^{-1} \cdot \boldsymbol{K} \ . \quad (3)$$

And the cost function $C(X)$ is given by:

$$C(X) = [\big(\boldsymbol{Y} - \boldsymbol{F}(X)\big)^T \cdot \boldsymbol{S}_e^{-1} \cdot \big(\boldsymbol{Y} - \boldsymbol{F}(X)\big) + (\boldsymbol{X} - \boldsymbol{X}_a)^T \cdot \boldsymbol{S}_a^{-1} \cdot (\boldsymbol{X} - \boldsymbol{X}_a)]/n_y \ , \quad (4)$$

where $\boldsymbol{F}$ is the forward model, $\boldsymbol{Y}$ is a series of observations value, $\boldsymbol{X}$ is the state of the atmosphere, $\boldsymbol{S}_e$ is the covariance matrix of the observation error and $\boldsymbol{K}$ is the matrix of weighting function. The a priori state vector is denoted by $\boldsymbol{X}_a$, with its covariance matrix $\boldsymbol{S}_a$ And n_y is the number of $\boldsymbol{Y}$ vector.

In our retrieval scheme, retrieval experiments are made based on many simulated spectra and ACE-FTS observation data to decide an optimal choice of γ. After statistical analysis, the factor of γ is defined as a linear scaled function to the cost function. It will be updated at each iteration, which is given by the following equation. Here, a is a constant and it is different for different atmospheric species.

$$\gamma_i = a \cdot C(\boldsymbol{X}_i) \ . \quad (5)$$

The definition of the a priori covariance matrix $\boldsymbol{S}_a$ follows Gaussian statistics and considers the correlation between different components of the state vector and the forward model vector. Different types of the correlation function [24] for computing the correlation have been tested based on the retrievals from simulated and observed ACE-FTS data. In this study, we employ the linear correlation function:

$$\boldsymbol{S}_a(i,j) = \max\{0, \sigma(i)\sigma(j)\left[1 - (1-e^{-1})\frac{2|z(i)-z(j)|}{lc(i)-lc(j)}\right]\} \ , \quad (6)$$

where i and j are position indexes, z is the position, lc is the correlation length and $|*|$ signifies the absolute value. σ is the standard deviation calculated from the a priori.

In the retrieval scheme of AIUS, we adopt the "dx" in the Qpack 2.0 as the threshold of convergence. The iteration is considered converged in the condition that the value of dx is smaller than 0.01. The definition of dx is that:

$$dx = [(\boldsymbol{X}_{i+1} - \boldsymbol{X}_i)^T \cdot \boldsymbol{S}_x^{-1} \cdot (\boldsymbol{X}_{i+1} - \boldsymbol{X}_i)]/n_x \ , \quad (7)$$

where n_x is the length of the state vector.

Preprints (www.preprints.org) | NOT PEER-REVIEWED | Posted: 20 April 2018 doi:10.20944/preprints201804.0257.v1

3.2 Adopted forward model

An accurate modeling of the radiative transfer through the atmosphere plays an important role in the inversion. The forward model adopted in the retrieval algorithm of AIUS is the RFM (Reference Forward Model) with the latest release version v4.36 [25]. RFM is a GENLN2-based line-by-line radiative transfer model originally developed at AOPP, Oxford University, under an ESA contract to provide reference spectral calculations for the MIPAS (The Michelson Interferometer for Passive Atmospheric Sounding) instrument launched on the ENVISAT (Environmental Satellite) in 2002. It has been subsequently developed into a general purpose code suitable for a variety of different spectroscopic calculations. Von Clarmann [26] has compared five forward models including the RFM. The inter-comparison experiment showed that the overall inter-consistency of spectra for all participants is good, which also can demonstrate that the RFM works fine and reliable.

RFM can deal with various measurement conditions including nadir viewing, limb sounding, occultation observation from different platforms (satellite /balloon /aircraft). Its main features are listed below:

1. It has high flexibility when defining observation geometry (including scanning features) and sensor characteristics.
2. It can provide Jacobians for p, T, VMR, line-of-sight pointing and surface temperature and emissivity.
3. Cross sections can be computed from HITRAN (High-resolution Transmission) spectroscopic database or read from external files.
4. Continua for H_2O, O_2, N_2 and CO_2 are included [27-31].

For all considered microwidows, scattering can be negligible and is not taken into accout in our retrieval scheme.

3.3 Microwindows

The spectral resolution of AIUS is about 0.02 cm-1. Because of this, the number of data points from each absorption band becomes unrealistic for an efficient inversion process. Furthermore, one should avoid the effect of interfering species on the retrieval of the target species and have the best information on the retrieval. Thus, the retrieval is performed using a set of narrow spectral interval (called "microwindow") instead of an entire spectral band.

To select an appropriate set of microwindows, a sensitivity analysis with Jacobians is required. First of all, we select the spectral points which are sensitive to the target gas on each cutting height and are not sensitive to the interference gas according to the Jacobians of target and the interference species. Then, the selected spectral points are grown on the basis of information entropy to generate a series of continuous window. Finally, all the selected microwindows at different tangent height are combined.

The absorption lines of O_3 in the infrared band are mainly located near 9.6 μm and the main interfering gases of O_3 in this spectral band include CO_2, H_2O and N_2O. The chosen microwindows for O_3 retrieval are shown in Figure 1. For O_3 retrieval, about 20 microwindows are selected, covering from 5 km to 95 km. Microwindows in the range of 1000--1070 cm^{-1} are sensitive at higher altitudes, while others are sensitive at lower altitudes.

Preprints (www.preprints.org) | NOT PEER-REVIEWED | Posted: 20 April 2018 doi:10.20944/preprints201804.0257.v1

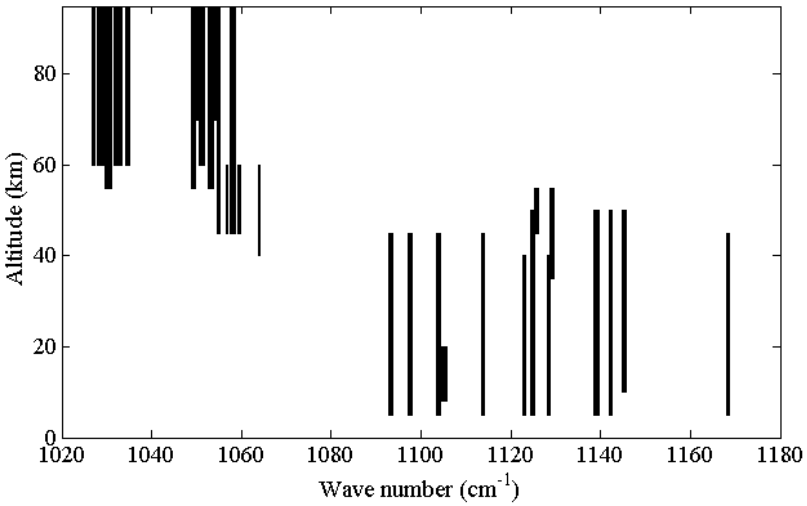

Figure 1 The microwindows selected for O_3 retrieval.

4. Sensitivity analysis of atmospheric profiles in forward model

4.1 Integrated Atmospheric profiles

The forward model generates a numerical simulation of measurements based on the given atmospheric state. In other words, the accuracy of the simulated measurements depends on the reliability of the atmospheric parameters used in the forward model. In our retrieval scheme, we compute a dataset of integrated atmospheric profiles based on MLS (Microwave Limb Sounder) level 2 products, ACE-FTS level 2 products and the profiles from AFGL(Air Force Geophysics Laboratory) atmospheric models.

The ACE-FTS level 2 v3.6 and the MLS level 2 (v4.2) products between 2014 and 2016 are considered. We classify and store the species profiles month by month for each set of products. Then, the monthly mean profiles are acquired and classified into different coordinate grids, which is discretized with a 5° latitude and 30° longitude spacing.. That is, both of two set of dataset are classified by month and coordinate grid. A diagram of constructing the integrated atmospheric profiles is shown in Figure 2.

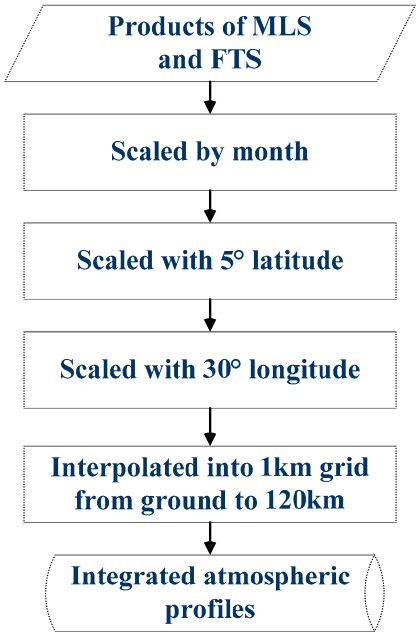

Figure 2 The technological process of constructing the integrated atmospheric profiles.

Preprints (www.preprints.org) | NOT PEER-REVIEWED | Posted: 20 April 2018 doi:10.20944/preprints201804.0257.v1

The next step is to combine the two sets of profiles. Since ACE-FTS and AIUS have similar instrument characteristics, the ACE-FTS product is chosen in case that the profile of a particular species at the same geolocation and time can be found in both ACE-FTS and MLS datasets. Finally, profiles of the missing species are read from the AFGL dataset. The species profiles imported from AFGL dataset include NH_3, HBr, HI, PH_3, H_2S, F11, F12, F13, F21, F22, F114, F115 and HNO_4. These species profiles from FASCOD (Fast Atmospheric Signature Code) Model 1-6 are resampled and packed into the monthly geographic grids. In the end, the integrated atmospheric species profiles dataset is produced.

4.2 Data simulation and sensitivity analysis

A comparison between the integrated atmospheric and AFGL profiles is carried out by simulating the ACE-FTS spectra. The simulation is made with the geolocation and geometry parameters of the ACE-FTS instrument. Figures 3 and 4 compare the simulated ACE-FTS using the two atmospheric profiles database to the observed spectra in two spectra ranges.

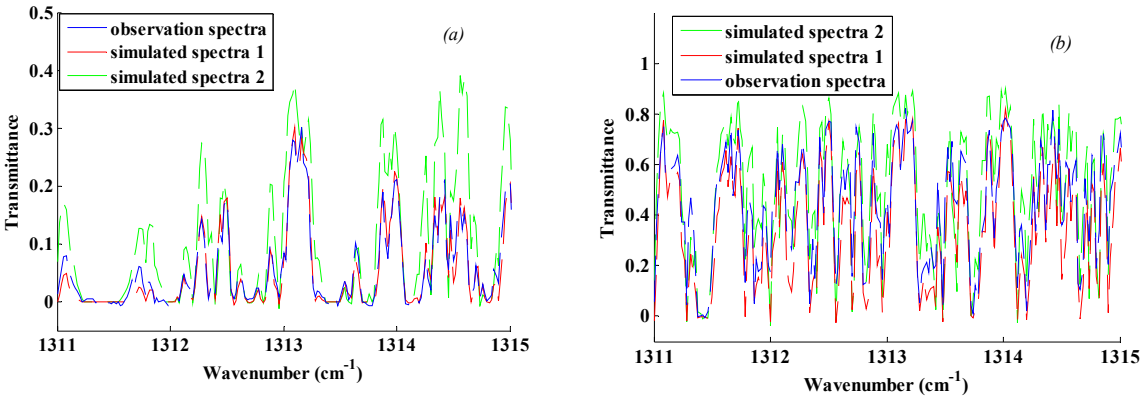

Figure 3 Comparison experiment between the integrated atmospheric and AFGL profiles (67.5°S, 72.5°W, August 5, 2012). (a) Tangent height=10.71 km; (b) Tangent height=20.48 km.

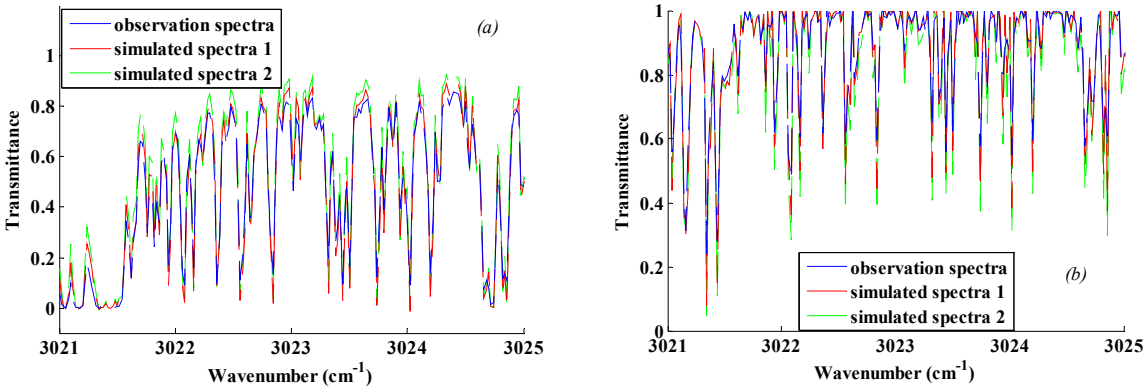

Figure 4 Comparison experiment between the integrated atmospheric and AFGL profiles (77°S, 86°E, March 25, 2012). (a) Tangent height=16.16 km; (b) Tangent height=30.4 km.

The simulated spectra 1 and 2 stand for the ones using the integrated atmospheric and AFGL profiles, respectively. Figures 3 and 4 show that in both spectral ranges, the simulated spectra using the integrated atmospheric profiles are obviously more close to the ACE-FTS observed spectra than those using the AFGL atmospheric profiles. The two comparison experiments demonstrate that the simulated spectra are very sensitive to the atmospheric profiles and that the simulated spectra using the dataset of integrated atmospheric profiles agree well to the actual measurements.

Preprints (www.preprints.org) | NOT PEER-REVIEWED | Posted: 20 April 2018 doi:10.20944/preprints201804.0257.v1

5. O_3 retrieval and assessment

5.1 Assessment of retrieval algorithm based on simulated spectra

Table 1 Retrieval configuration

Parameters	Retrieval configuration
spectroscopic database	Hitran 2012 [32]
continua used	O_2, H_2O, N_2
Retrieval altitude grids /km	8 10 12 15 17 20 25 30 35 40 45 50 55 60 65 70 75 80 85 90
altitude grids in the forward model	0-100 km with 1 km resolution
O3 true profiles (X_true)	Taken from integrated atmospheric database
$\boldsymbol{X_a}$	$0.8 \cdot \boldsymbol{X\_true}$

The O_3 retrieval performance is first assessed by using simulated measurements. The microwindows selected in section 3.3 are adopted. Two O_3 profiles picked from two grids of the integrated atmospheric dataset (75°S, 150°W in October and 65°S, 90°E in March) are taken as the true profiles to simulate spectra of AIUS. Then, the artificial noise with SNR = 300 is added to the simulated spectra. Details of retrieval configuration are specified in Table 1. The retrieved profiles are shown in Figure 5 and 6.

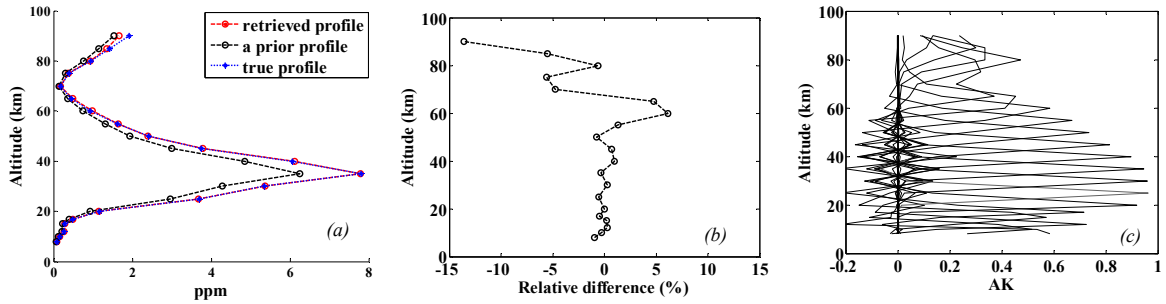

Figure 5 O_3 retrieval experiment based on simulated spectra at 75°S, 150°W in October. (a)Retrieved profile; (b) Relative difference between retrieved and true profiles; (c) Averaging kernel.

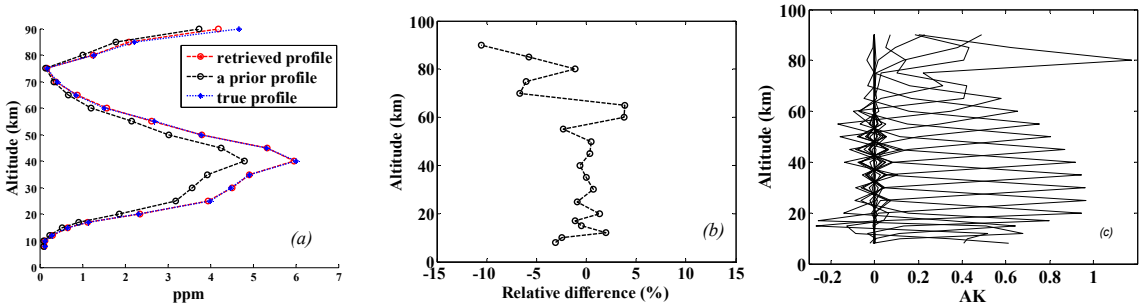

Figure 6 O_3 retrieval experiment based on simulated spectra at 65°S, 90°E in March. (a)Retrieved profile; (b) Relative difference between retrieved and true profile; (c) Averaging kernel.

The a priori, true profile and retrieval profile of O_3 are shown in figure 5(a) and 6(a). The shape and the values of retrieval profiles are consistent with the true profiles. The relative difference between the retrieval and true profiles presented in figure 5(b) and 6(b) shows that it is within ±5% below 60 km, within ±7% from 60 km to 80 km. The averaging kernels in figure 5(c) and 6(c) illustrate that the retrieval information mainly comes from the measurements.

Preprints (www.preprints.org) | NOT PEER-REVIEWED | Posted: 20 April 2018 doi:10.20944/preprints201804.0257.v1

As the residual in both experiments seems nearly identical, only the one in the first experiment is shown in Figure 7.The lowest to the highest tangent heights is from left to right. The residuals at each tangent height are within ±0.02, which are very small.

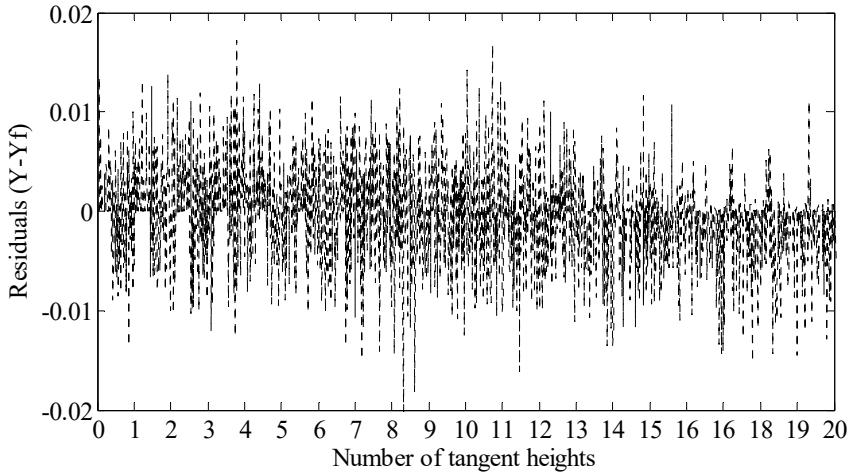

Figure 7 The residuals of the first retrieval experiment.

In the above retrieval experiments, $\boldsymbol{X}_a = 0.8 \cdot \boldsymbol{X\_true}$, but the shape is same. Thus, more retrieval experiments are made to assessment the dependence of the AIUS algorithm on the shape of the a prior profile. In this experiment, the ACE-FTS O_3 level 2 products are taken as the true profiles. The information of five products selected is shown in table 2. The a prior profiles are from the mean monthly profiles of MLS O_3 level 2 products, which indicates that the shape of the a prior profiles can be different from that of the true profiles.

Table 2 Information of O3 L2 products from ACE-FTS.

Scene ID	latitude	longitude	date
40993	-78	87	2012-3-25
39926	-68	131	2011-1-11
38154	63	-73	2010-9-13
43544	63	75	2011-9-14
43611	70	-119	2011-9-18

Similarly, the artificial noise with same SNR is added randomly to the simulated spectra. O_3 retrieval is performed and the results for these five retrieval experiments are similar. Thus, only results of two retrieval experiments using the O3 products from scenes of 40993 and 38154 are presented in Figures 8 and 9, respectively. The two scenes are located in Antarctica and Arctic, respectively.

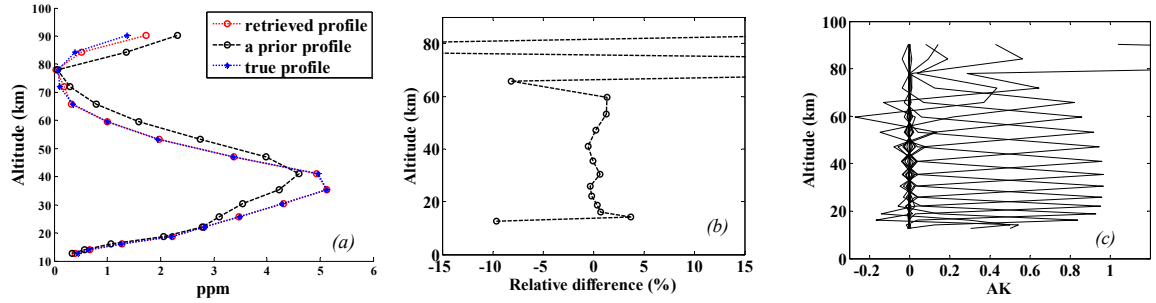

Figure 8 O_3 retrieval experiment based on O_3 product from scene 40993 of ACE-FTS. (a)Retrieved profile; (b) Relative difference between retrieved and true profile; (c) Averaging kernel.

Preprints (www.preprints.org) | NOT PEER-REVIEWED | Posted: 20 April 2018 doi:10.20944/preprints201804.0257.v1

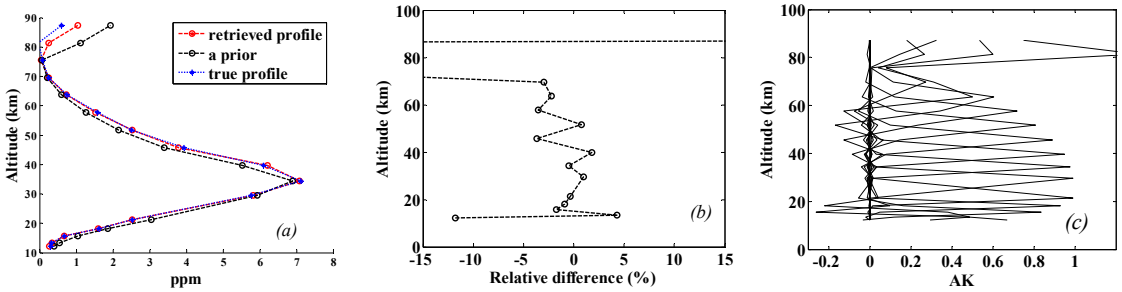

Figure 9 O_3 retrieval experiment based on O_3 product from scene 38154 of ACE-FTS. (a)Retrieved profile; (b) Relative difference between retrieved and true profile; (c) Averaging kernel.

Figures 8(a) and 9(a) show that the shape of the retrieval profiles is almost the same with the true profiles even that the shape of the a prior profiles is different from that of the true profiles. Figures 8(b) and 9(b) illustrate that the relative difference between the retrieval O_3 profiles and the true O_3 profiles is almost within 5% from 10 km to 70 km, about 10% near 10 km. However, the relative difference will reach beyond 30%. The reasons may be due to the low concentration of O_3 profiles and the retrieval above 70 km is dominated by the a priori information The averaging kernels in Figures 8(c) and 9(c) are similar as those in Figures 5(c) and 6(c), which indicate that the retrieval information mainly comes from the measurement in the troposphere and stratosphere. We also check the residuals of these five retrieval experiments, which are consistent with the residuals in Figure 7. All residuals of these five retrieval experiments are within ±0.02.

The retrieval experiments using synthetic AIUS spectra demonstrate that the algorithm produces reasonable results and sufficient retrieval sensitivity.

5.2 O3 retrieval based on ACE-FTS measurements

Under real-world conditions, in addition to the thermal noise of the instrument, the actual measurements are influenced by more factors. To evaluate the influence of various uncertainties on the retrieval algorithm of AIUS, we adopt the level 1 products of ACE-FTS to perform the O_3 retrieval experiments, as AIUS expects to perform measurements with similar characteristics. All the a prior profiles of O_3 and other species are taken from the dataset of integrated atmospheric profiles. The level 1products used are those five scenes of ACE-FTS observation data in table 2. Since the results for these five retrieval experiments are similar, only results of two retrieval experiments from scene 40993 and 38154 are presented.

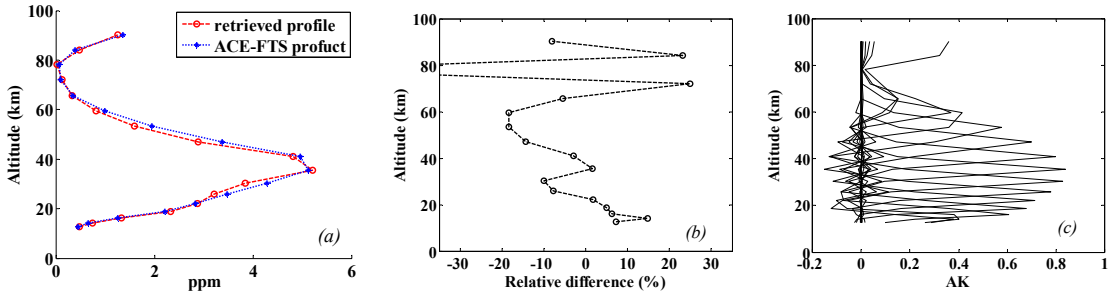

Figure 10 O_3 retrieval experiment based on FTS observation spectra from scene 40993. (a)Retrieved profile; (b) Relative difference between retrieved and FTS level 2 product; (c) Averaging kernel.

Preprints (www.preprints.org) | NOT PEER-REVIEWED | Posted: 20 April 2018 doi:10.20944/preprints201804.0257.v1

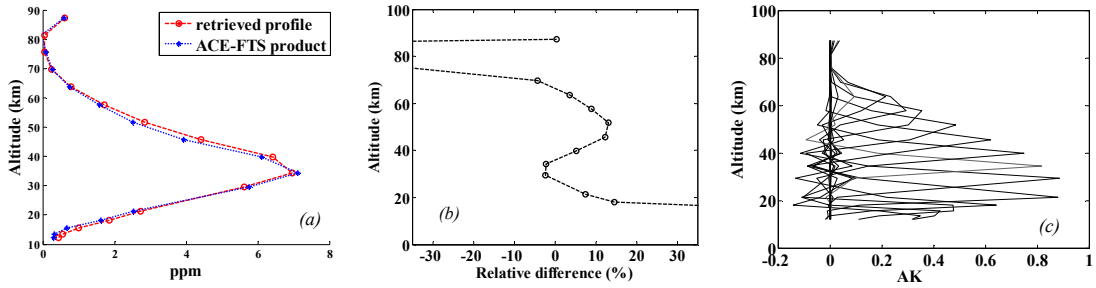

Figure 11 O_3 retrieval experiment based on FTS observation spectra from scene 38154. (a)Retrieved profile; (b) Relative difference between retrieved and FTS level 2 product; (c) Averaging kernel.

The retrieval profiles, the relative difference and averaging kernels are shown in figure 10 and 11. The retrieval profiles presented in figure 10(a) and 11(a) show that the shape of the retrieval O_3 profiles agree well to those of ACE-FTS level 2 products. However, the relative difference in figure 10(b) and 11(b) is bigger than that in figure 8(b) and 9(b). The relative difference of these two retrieval experiment below 70 km is mainly within 10%, with some points reach 15%-20%. The relative difference here is larger mainly because of the uncertainties in the measurements and different forward model parameters. The bias of the ACE-FTS O_3 products is +1 to +8% in the stratosphere (16–44 km) and can be up to +40% (+20% on average) above 45 km (Jones A., et al., 2012; Dupuy E., et al., 2009). Although the averaging kernels in Figures 10(c) and 11(c) are somewhat broader than those in Figures 8(c) and 9(c), it still reveals that the retrieval information mainly comes from the measurement in the stratosphere. The statistical analysis of the residuals demonstrate that about 90% residuals are within ±0.02, with some points reaching ±0.06, demonstrating the retrieval fits very well. Our algorithm dedicated to AIUS performs stable and delivers comparable results using ACE-FTS real measurements.

6. Discussion and conclusions

In this study, we have introduced a retrieval algorithm developed for an infrared occultation spectrometer called AIUS. The retrieval algorithm comprises a forward model based on RFM and an OEM framework adapted from Qpack, which employs the LM iteration method. The retrieval experiments of ozone retrievals were carried out based on simulated spectra and ACE-FTS measurements.

In the condition of experiments on simulated spectra, there are some differences depending on the profile shape of the a prior. When the shape of the a prior is the same as the true profile, the relative difference between the retrieval profile and the true profile is within ±5% below 60 km and within 7% in the range of 60-80 km. When the shape of the a prior is and the true profile is different, the retrieval profile shape still keep close to the true profile. The relative difference is a litter bigger. It is mainly within 5% below 60 km, but can reach 10% near 10 km and 10-15% from 60 km to 70 km. However, the relative difference is in a reasonable range. And the averaging kernels achieved illustrate that the retrieval information mainly comes from the simulated observation spectra. Thus the retrieval experiments based on simulated spectra indicate that the retrieval algorithm of AIUS work fine and successful.

When it comes to experiments based on ACE-FTS observation data, the retrieval algorithm of AIUS also behaves well. The retrieval experiments show that the relative differences between them are greater than those in the retrieval experiments using simulated spectra. The greater relative differences may be produced by the following reasons. Firstly, although the instrument parameters AIUS and FTS are similar, there must be different in some of the details. Thus, some errors will be brought by using ACE-FTS observation spectra as the AIUS observation spectra. Secondly, the ACE-FTS levels are not the true profiles. They also have uncertainties, which will make the relative difference greater. The last and the most important reason is the greater uncertainty of the observed spectra, which will generate some errors between the simulated spectra by the forward model and

Preprints (www.preprints.org) | NOT PEER-REVIEWED | Posted: 20 April 2018 doi:10.20944/preprints201804.0257.v1

the observation spectra in the retrieval process. Nevertheless, the retrieval profiles still agree well with the ACE-FTS level 2 products and the range of the relative differences is satisfactory.

All the retrieval experiments based on the simulated spectra and the measured spectra of ACE-FTS indicate that the retrieval algorithm of AIUS is reliable and robust. Overall, the retrieval profiles agree well with the true profiles or the ACE-FTS level 2 profiles. However, the uncertainties of the retrieval profiles at lower tangent height are still requiring further investigations. After the instrument is launched, we will improve the retrieval algorithm by fine-tuning the forward model parameters according to the characteristics of the AIUS observed spectra and the instrument performance. In addition, an extensive retrieval error characterization is on-going and will be consolidated during the operational phase.

Acknowledgments: This study was supported in part by the project 41571345 supported by National Natural Science Foundation of China, the National Key Research and Development Program of China (Grant No. 2016YFB0500705), the project supported by the Special Foundation for Free Exploration of State Laboratory of Remote Sensing Science (Grant No. Y1Y00202KZ), and the project supported by Major Projects of High Resolution Earth Observation System (Grant No. 32-Y20A18-9001-15-17-1). The ACE-FTS data were provided by ACE-FTS team. ACE, also known as SCISAT, is a Canadian-led mission mainly supported by the Canadian Space Agency (CSA). And Thanks to Professor Anu Dudhia for providing the RFM source code and help.

Author Contributions: Xiaoying Li, Tianhai Cheng and Jian Xu conceived and designed the experiments; Mingmin Zou, Hongmei Wang, Yapeng Wang, Songyan Zhu and Jing Miao performed the experiments; Xiaoying Li, Tianhai Cheng, Jian Xu, Hailiang Shi, Xingying Zhang and Shule Ge analyzed the data; Xiaoying Li wrote the paper.

Preprints (www.preprints.org) | NOT PEER-REVIEWED | Posted: 20 April 2018 doi:10.20944/preprints201804.0257.v1

References

1. Manney, G.L.; Santee, M.L.; Livesey, N.J.; Froidevaux, L.; Read, W.G.; Pumphrey, H.C.; Waters, J.W.; Pawson, S. EOS Microwave Limb Sounder observation of the Antarctic polar vortex breakup in 2004. *Geophysical Research Letters*. **2005**, *32(L12811)*, 1-5, DOI: 10.1029/2005GL022823.
2. Santee, M.L.; Manney, G.L.; Livesey, N.J.; Froidevaux, L.; MacKenzie, I.A.; Pumphrey, H.C.; Read, W.G.; Schwartz, M.J.; Waters, J.W.; Harwood, R.S. Polar processing and development of the 2004 Antarctic ozone hole: First results from MLS on Aura. *Geophysical Research Letters*. **2005**, *32(L12817)*, 1-4, DOI: 10.1029/2005GL022582.
3. Gattinger, R. L.; McDade, I. C.; Alfaro Suzan, A. L. ; Boone, C. D.; Walker, K.A.; Bernath, P.F.; Evans, W.F. J.; Degenstein, D.A.; Yee, J.-H.; Sheese, P.; Llewellyn, E. NO_2 air afterglow and O and NO densities from Odin-OSIRIS night and ACE-FTS sunset observations in the Antarctic MLT region. *Journal of Geophysical Research*. **2010**, *115 (D12)* , 1256-1268, DOI: 115. 10.1029/2009JD013205.
4. Russell, J.M.; Gordley, L.L.; Park, J.H.; Drayson, S.R.; Hesketh, W.D.; Cicerone, R.J.; Tuck, A.F.; Frederick, J.E.; Harries, J.E.; Crutzen, P.J. The Halogen Occultation Experiment. *Journal of Geophysical Research-Atmospheres*. **1993**, *98(D6)*, 10777-97.
5. Gunson, M.R.; Abbas, M.M.; Abrams, M.C.; Allen, M.; Brown, L.R.; Brown, T.L.; Chang, A.Y.; Goldman, A.; Irion, F.W.; Lowes, L.L.; Mahieu, E.; Manney, G.L.; Michelsen, H.A.; Newchurch, M.J.; Rinsland, C.P.; Salawitch, R.J.; Stiller, G.P.; Toon, G.C.; Yung, Y.L.; Zander, R. The Atmospheric Trace Molecule Spectroscopy (ATMOS) experiment: Deployment on the ATLAS Space Shuttle missions. *Geophysical Research Letters*. **1996**, *23(17)*, 2333-2336.
6. Bovensmann, H.; Burrows, J.P.; Buehwitz, M.; Frerick, J.; Noel, S.; Rozanov, V.V. SCIAMACHY: Mission Objectives and Measurement Modes. *Journal of the atmospheric sciences*. **1999**, *56(2)*, 127-150.
7. Beer, R.; Glavich, T.A.; Rider, D.M. Tropospheric emission spectrometer for the Earth Observing System's Aura Satellite. *Applied Optics*. **2001**, *40(15)*, 2356-67.
8. Bernath P.F.; McElroy C.T.; Abrams M.C.; Boone, C.D.; Butler, M.; Camy-Peyret, C.; Carleer, M.; Clerbaux, C.; Coheur, P.-F.; Colin, R.; DeCola, P.; DeMazie`re, M.; Drummond, J. R.; Dufour, D.; Evans, W. F. J.; Fast, H.; Fussen, D.; Gilbert, K.; Jennings, D.E.; Llewellyn, E. J.; Lowe, R.P.; Mahieu, E.; McConnell, J.C.; McHugh, M.; McLeod, S.D.; Michaud, R.; Midwinter, C.; Nassar, R.; Nichitiu, F.; Nowlan, C.; Rinsland, C.P.; Rochon, Y.J.; Rowlands, N.; Semeniuk, K.; Simon, P.; Skelton, R.; Sloan, J.J.; Soucy, M.-A.; Strong, K.; Tremblay, P.; Turnbull, D.; A. Walker, K. ; Walkty, I.;. Wardle, D.A; Wehrle, V.; Zander, R., Zou, J. Atmospheric Chemistry Experiment (ACE): Mission overview. *Geophysical Research Letters*. **2005**, 32, L15S01, doi:10.1029/2005GL022386.
9. Fischer, H.; Birk, M.; Blom, C.; Carli, B.; Carlotti, M.; Clarmann, T.von; Delbouille, L.; Dudhia, A.; Ehhalt, D.; Endemann, M.; Flaud, J.M.; Gessner, R.; Kleinert, A.; Koopman, R.; Langen, J.; Lopez-Puertas´, M.; Mosner, P.; Nett, H.; Oelhaf, H.; Perron, G.; Remedios, J.; Ridolfi, M.; Stiller, G.; Zander, R.. MIPAS: an instrument for atmospheric and climate research. *Atmos Chem Phys*. **2008**, *8(8)*, 2151-88.
10. Rodgers, C.D. Retrieval of atmospheric temperature and composition from remote measurements of thermal radiation. *Reviews of Geophysics and Space Physics*. **1976**, *14(4)*, 609-624.
11. Urban, J.; Baron, P.; Lautie, N.; Schneider, N.; Dassas, K.; Ricaud, P.; de la Noë, J. Moliere (v5): a versatile forward- and inversion model for the millimeter and sub-millimeter wavelength range. *Journal of Quantitative Spectroscopy and Radiative Transfer*. **2004**, *83(3/4)*, 529-554, DOI: 10.1016/S0022-4073(03)00104-3.
12. Boone, C.D.; Nassar, R.; Walker, K.A.; Rochon, Y.; McLeod, S.D.; Rinsland, C.P.; Bernath, P.F. Retrievals for the atmospheric chemistry experiment Fourier-transform spectrometer. *Applied Optics*. 2005, *44(33)*, 7218-31.
13. Raspollini, P.; Belotti, C.; Burgess, A.; Carli1, B.; Carlotti, M.; Ceccherini, S.; Dinelli, B.M.; Dudhia, A.; Flaud, J.-M.; Funke, B.; Hopfner, M.; Lopez-Puertas, M.; Payne, V.; Piccolo, C.J.; Remedios, J.; Ridolfi, M.; Spang, R. MIPAS level 2 operational analysis. *Atmos. Chem. Phys.***2006**, *6*, 5605–5630.
14. Livesey, N.J.; Snyder, W.V.; Read, W.G.; Wagner, P. A. Retrieval Algorithms for the EOS Microwave Limb Sounder (MLS). *IEEE Transactions on Geoscience and Remote Sensing*. **2006**, *44(5)*, 1144-1155.
15. Bowman, K.W.; Rodgers, C.D.; Kulawik, S.S.; Worden, J.; Sarkissian, E.; Osterman, G.; Steck, T.; Lou, M.; Eldering, A.; Shephard, M.; Worden, H.; Lampel, M.; Clough, S.; Brown, P.; Rinsland, C.; Gunson, M.; Beer, R. Tropospheric Emission Spectrometer: Retrieval Method and Error Analysis. *IEEE Transactions on Geoscience and Remote Sensing*. **2006**, *44(5)*, 1297-1307.

Preprints (www.preprints.org) | NOT PEER-REVIEWED | Posted: 20 April 2018 doi:10.20944/preprints201804.0257.v1

16. Takahashi, C.; Ochiai, S.; Suzuki, M. Operational retrieval algorithms for JEM/SMILES level 2 data processing system. *Journal of Quantitative Spectroscopy & Radiative Transfer*. **2010**, *111*, 160–173.
17. Rodgers, C.D. *Inverse Methods for Atmospheric Sounding: Theory and Practice, Series on Atmospheric Oceanic and Planetary Physics-Vol. 2*, World Scientific Publishing Co. Pte. Ltd: P O Box 128, Farrer Road, Singapore, 2000; pp. 92-93, ISBN: 981-02-2740-X.
18. Eriksson, P. Analysis and comparison of two linear regularization methods for passive atmospheric observations. *Journal of Geophysical Research*. **2000**, *105(D14)*, 18,157-18,167.
19. Doicu, A.; Schreier, F.; Hess, M. Iteratively regularized Gauss – Newton method for atmospheric remote sensing. *Computer Physics Communications*. **2002**, *148*, 214–26.
20. Steck, T. Methods for determining regularization for atmospheric retrieval problems. *Applied Optics*. **2002**, *41(9)*, 1788-1797.
21. Jiang, D.M.; Dong, C.H. A review of optimal algorithm for physical retrieval of atmospheric profile. *Advances in Earth Science*. **2010**, *25(2)*, 133-139.
22. Zou, M.M.; Chen, L.F.; Li, S.S.; Fan, M.; Tao, J.H.; Zhang, Y. An improved constraint method in optimal estimation of CO2 from GOSAT SWIR observations. *Science China Earth Sciences*. **2016**, DOI: 10.1007/s11430-015-0247-9.
23. Xu, J.; Schreier, F.; Doicu, A.; Trautmann, T. Assessment of Tikhonov-type regularization methods for solving atmospheric inverse problems. *Journal of Quantitative Spectroscopy & Radiative Transfer*. **2016**, *184*, 274–286.
24. Eriksson, P.; Jimeneza, C.; Buehler, S.A. Qpack, a general tool for instrument simulation and retrieval work. *Journal of Quantitative Spectroscopy & Radiative Transfer*. **2005**, *91*, 47-64.
25. REFERENCE FORWARD MODEL. Available online: http://eodg.atm.ox.ac.uk/RFM/index.html.
26. Von Clarmann, T..; Hopfner, M.; Funke, B.; Lopez-Puertas, M.; Dudhia, A.; Jay, V.; Schreier, F.; Ridolfi, M.; Ceccherini, S.; Kerridge, B.J.; Reburn, J.; Siddans, R. Modelling of atmospheric mid-infrared radiative transfer: the AMIL2DA algorithm intercomparison experiment. *Journal of Quantitative Spectroscopy & Radiative Transfer*. **2003**, *78*, 381-407.
27. Clough, S.A.; Kneizys, F.X.; Davies, R.W. Line shape and the water vapor continuum. Atmos. Res. **1989**, *23*, 229-241, DOI: 10.1016/0169-8095(89)90020-3.
28. Mlawer, E.J.; Payne, V.H.; Moncet, J.-L.; Delamere, J.S.; Alvarado, M.J.; Tobin, D.C. Development and recent evaluation of the MT-CKD model of continuum absorption. Philosophical Transactions of the Royal Society A: Mathematical, Physical and Engineering Sciences. **2012**, *370 (1968)*,. 2520-2556, DOI: 10.1098/rsta.2011.0295.
29. Thibault, F.; Menoux, V.; Le Doucen, R.; Rosenmann, L.; Hartmann, J.-M.; Boulet, Ch. Infrared collision-induced absorption by O2 near 6.4 μm for atmospheric applications: measurements and empirical modeling. *Appl. Opt.* **1997**, *36*, 563-567.
30. Lafferty, W.J.; Solodov, A.M.; Weber, A.; Olson, W.B.; Hartmann, J.-M. Infrared collision-induced absorption by N2 near 4.3 μm for atmospheric applications: measurements and empirical modeling. *Appl. Opt.* **1996**, *35*, 5911-5917.
31. .Clough, S.A.; Kneizys, F.X.; Rothman, L.S.; Gallery, W.O. Atmospheric Spectral Transmittance And Radiance: FASCOD1 B. *Proc. SPIE 0277, Atmospheric Transmission*. **1981**, *277(12)*, 152-166 DOI: 10.1117/12.931914.
32. Rothman, L.S.; Gordon, I.E.; Babikov, Y; Barbe, A.; Chris Benner, D.; Bernath, P.F.; Birk, M.; Bizzocchi, L.; Boudon, V.; Brown, L.R.; Campargue, A.; Chance, K.; Cohen, E.A.; Coudert, L.; Malathy Devi, V.; Drouin, B.; Fayt, A.; Flaud, J.-M.; Gamache, R.; Wagner, G. The HITRAN 2012 Molecular Spectroscopic Database. *Journal of Quantitative Spectroscopy and Radiative Transfer*. **2013**, *130*, 4-50.